BrAVe: a unified framework for 3D interactive and integrative analysis of cross-modal multi-scale brain atlas data in diverse species

Yu-Fan Wang[1], Ming-Quan Chen[1], Jia-Fei Wei[1], Hong-Bo Ma[1], Yong-Wei Zhong[1], Fu-Ning Li[1], Chen-Xi Jin[1], Si-Xuan Cheng[1,2], Jia-Qi Guan[1,2], Yuan-Ming Zheng[3], Tian-Lei Zhang[1], Chao Chen[1,2], Xiu-Dan Zheng[1], Sheng-Jin Xu[1,2], Kai Wang[1,2], Zhi-Feng Yue[1], Jiu-Lin Du[1,2,4,*] & Xu-Fei Du[1,2,*]

[1] Institute of Neuroscience, State Key Laboratory of Brain Cognition and Brain-Inspired Intelligence Technology, Center for Excellence in Brain Science and Intelligence Technology, Chinese Academy of Sciences, 320 Yue-Yang Road, Shanghai 200031, China

[2] University of Chinese Academy of Sciences, 19A Yu-Quan Road, Beijing 100049, China

[3] School of Life Science, Fudan University, Shanghai 200438, China

[4] School of Life Science and Technology, ShanghaiTech University, 393 Middle Huaxia Road, Shanghai 201210, China

* These authors jointly supervised this work: Jiu-Lin Du (forestdu@ion.ac.cn),
Xu-Fei Du (xufeidu@ion.ac.cn)

The brain exhibits remarkable complexity across molecular, structural, and functional modalities spanning spatial scales from micro- to macro-levels[1–3]. Recent advances in brain mapping have yielded increasingly sophisticated multimodal, multi-scale atlases in diverse species[4–26]. However, integrative analysis across these modalities and scales remains hindered by methodological and tool limitations[27]. Here, we present BrAVe (BrainAtlas Viewer), an open-source, species-agnostic framework for 3D visualized and integrative analysis of brain atlas data across modalities and scales. BrAVe supports five core data types—volumetric images, parcellated regions, feature points, neuronal tracings, and networks—in standard formats (e.g., .nrrd, .stl, .csv., and .swc), accommodating multimodal and multi-scale datasets from flies to primates. For single-modality datasets, BrAVe provides a suite of analyses, with regional distribution profiling as a common feature. This is exemplified by its single-neuron morphology analysis, which enables quantitative characterization of geometry, topology, projection, clustering, and putative wiring. For multimodal datasets, BrAVe establishes spatially resolved correspondence across modalities within a common reference space, allowing the identification of molecularly defined neurons and the discovery of functionally associated circuits. BrAVe further bridges scales by matching neuronal reconstructions from light microscopy (LM) and electron microscopy (EM), enabling assignment of LM neuronal types for EM datasets, and leveraging EM synaptic connectivity to refine mesoscale wiring. Additional features include 3D image registration, scalable client-server data handling, and export of static and animated outputs. Combined with its intuitive interface and species compatibility, BrAVe offers a unified solution for integrative analysis of brain atlas datasets and empowers data-driven discovery in neuroscience research.

A comprehensive understanding of the brain requires a holistic view of its molecular composition, structural architecture, and functional dynamics. Critically, these distinct types of information need to be presented and integrated within a common physical space to enable cross-modal analysis and interpretation[28]. For example, spatiotemporal patterns of brain-wide neuronal activity can be understood when contextualized by the underlying anatomical connectivity among regions and constituent neurons. Technological advances have enabled the generation of multimodal brain atlas datasets at multiple spatial scales, increasingly spanning developmental stages and diverse species[4–26]. Unlocking the potential of these large-scale efforts requires user-friendly tools that can integrate, interrogate, and analyze multimodal, multi-scale data within a coherent three-dimensional (3D) spatial reference.

High-resolution 3D reference brain atlases have been established for major model organisms[10,11,14,29–35], offering standardized anatomical coordinate frameworks for spatial alignment of diverse datasets from micro- to macroscopic scales. Complementary advances in image registration pipelines have further accelerated atlas-based data integration[36–40]. Building

on these foundations, a growing ecosystem of atlas-centered web or software platforms has emerged. Initial web-portal efforts in the mouse field emphasized specific brain organizations, such as cell-type cytoarchitecture in the Blue Brain Cell Atlas[41] and single-neuron reconstructions in the MouseLight NeuronBrowser[17]. In parallel, web-based portals were developed to provide community access to atlas datasets in other model systems, such as mapzebrain for zebrafish[11] and Virtual Fly Brain for *Drosophila*[42]. Alongside these species-specific portals, standalone tools were developed to address common analytical needs: NeuTube supports visualization of SWC neuronal reconstructions[43], WholeBrain enables segmentation, registration, and neuroanatomical analysis of light-microscopy images[44], and the natverse toolkit provides quantification and clustering of neuronal morphologies[45]. Moving a step further, Brainrender[46] enables 3D rendering of multiple atlas-registered data, including regions, points, and neuronal tracings. Locare[47] introduces a standardized workflow to represent heterogeneous neuroscience data as geometric objects in 3D atlases, enabling co-visualization of multimodal datasets within a shared coordinate framework.

These efforts together illustrate a transition from specialized tools tailored to single modalities or species toward frameworks that can accommodate datasets across modalities and species, and from static data exploration to spatially resolved analyses. Despite these advances, a major challenge remains: developing platforms that enable integrative analyses of brain atlas datasets across modalities, scales, and species, thereby supporting holistic understanding of brain structure and function[27].

To address this, we developed the BrainAtlas Viewer (BrAVe), an open-source software platform for 3D interactive and integrative analysis of multimodal and multi-scale brain atlas data. BrAVe supports five core data types: volumetric images, parcellated regions, spatial feature points, neuronal skeletons, and connectivity networks. These data types collectively provide a comprehensive framework for representing the molecular, structural, and functional dimensions of brain atlas data across micro-, meso-, and macroscopic scales. For each type, BrAVe offers dedicated visualization and spatially resolved quantification. Once datasets are registered to a common reference atlas, BrAVe enables cross-modal integration with evaluation based on spatial relationships, irrespective of the data origin and format. For example, users can interactively relate gene expression patterns or brain-wide neural activities to morphologies of specific neurons, and further examine those neurons' projection patterns and putative neural circuits, all within a unified interface. It further links scales through correspondence of neuronal reconstructions obtained with light microscopy (LM) and electron microscopy (EM), transferring neuronal identity from LM to EM data and neural connectivity from EM to LM data. These functions together enable joint analyses throughout the entire hierarchy of brain organization.

To extend applicability, BrAVe includes built-in registration module for aligning unregistered datasets to species-specific reference templates. The platform is powered by a high-performance backend infrastructure that ensures real-time rendering and smooth

interaction with large-scale datasets, such as whole-brain neuron reconstructions and synaptic-resolution connectomes. The platform also features usability, demonstrated by an intuitive user interface and a context-sensitive right-click menu within the 3D *RenderView*, enabling direct interaction with data objects and streamlined access to core visualization and analytical functions. BrAVe facilitates data sharing and reproducibility through standardized metadata encoding (JSON) and exportable analytical outputs in Excel format. In addition, it supports high-quality export of static images and user-defined animations, facilitating effective scientific communication. Moreover, it allows users to incorporate custom algorithms and adapt the platform to emerging data types or analytical needs.

Taken together, BrAVe offers an all-in-one solution for interactive and integrative analysis of brain atlas data across modalities and scales in diverse species. By bridging molecular, structural, and functional domains through spatial contexts, BrAVe provides an essential foundation for data-driven discovery in neuroscience research.

System architecture of the BrAVe platform

Mapping brain atlas efforts have generated increasingly diverse, large-scale datasets across experimental paradigms, data modalities, and species. However, these resources often remain fragmented as isolated data silos, and effective use of them is often restricted to individual research groups with advanced computational expertise. In developing BrAVe, we aimed to overcome these barriers through two guiding design principles. First, we sought to enable spatially grounded integration across diverse datasets registered into a common coordinate space, thereby breaking inter-dataset isolation and fostering cross-modal correspondence. Second, we prioritized accessibility, ensuring that experimenters, regardless of programming experience, could intuitively explore, analyze, and interpret complex 3D brain datasets. To achieve these, we evaluated existing open-source solutions and selected ParaView[48] as a prototype system, given its strengths in 3D rendering, spatial queries, and scalable data handling. BrAVe extends this architecture with neuroscience-specific functionalities to support single-modal, cross-modal, and cross-scale brain atlases' interactive visualized analysis and integration (Fig. 1).

The first essential step was to standardize the import and representation of heterogeneous datasets across species. Despite methodological diversity, most brain atlas data fall into three principal modalities—molecular, structural, and functional—each represented at microscopic (synaptic), mesoscopic (single-cell or cell-type), and macroscopic (brain region) scales. To accommodate this diversity, BrAVe was designed to ingest five applicable data types (Fig. 1a-I, and Fig. 1b): (1) volumetric images (.nrrd, .nii, .tif, .hdr), the primary format for raw data; (2) parcellated regions (.stl, .obj), 3D surfaces delineating brain regions or structures; (3) spatial feature points (.csv), specifying positions of gene expression, labeled cells or proteins, axon terminals, or functionally active neurons; (4) neuronal tracings (.swc), skeletonized reconstructions of individual neurons from LM and EM; and (5) connectivity networks (.csv),

source-target matrices describing interactions among neurons, neuronal types, or brain regions. Please note that .stl, .obj, .swc, and .csv files are digitized data derived from image datasets. This species-agnostic, source-independent framework enables integration of datasets spanning spatial transcriptomics, transgenic labeling, neuronal reconstructions from LM and EM, functional recordings such as calcium imaging or functional magnetic resonance imaging (fMRI), and multi-scale network maps.

Once loaded, datasets can be explored and analyzed through a modular graphical interface comprising multiple coordinated tools (Fig. 1a-II; see Methods). The *Pipeline Browser* and *Data Browser* serve complementary roles in data management. The *Pipeline Browser* organizes the processing workflow, enabling users to launch analysis modules (*Filters*) and adjust their parameters via the *Properties Panel*. The *Data Browser* focuses on the dataset itself, providing control over the visibility, sorting, and coloring of individual elements. The core rendering view in BrAVe is the 3D *RenderView*, which delivers spatially resolved visualization and direct user interaction. Quantitative analysis outputs are rendered within this view, such as coloring neurons according to the branch order (Fig. 1d-II). We created a *Context Menu* within the 3D *RenderView* to facilitate rapid toggling of object visibility, color customization, grouping, and export of analysis results. Crucially, it supports spatially driven interactions with the data: users can select objects directly in 3D space and dynamically retrieve mapped information, such as displaying presynaptic neurons of a chosen neuron (Fig. 1d-IV). The entire process is fully visualized, enabling transparent and intuitive data interrogation.

The analytical functions of BrAVe are implemented through the *Filters* module (Fig. 1a-II), which can be directly selected to apply or triggered via the *Context Menu*. These functions fall into three hierarchical categories (Fig. 1c): (1) intra-modal quantification, including general analysis (e.g., density and regional distribution) and modality-specific analysis (e.g., for the neuronal structural modality, BrAVe calculates morphological parameters and similarity, and estimates putative connections between individual neurons based on axon-dendrite proximity) (Fig. 1c, top right; see Fig. 3); (2) cross-modal mapping between molecular, structural, and functional data, linking gene expression profiles, neuronal morphology, and neural activity patterns based on spatial queries (Fig. 1c, bottom right; see Figs. 4,5); (3) cross-scale integration, by matching single-cell reconstructions from LM and EM data, thereby bridging microscopic connectivity with mesoscopic genetic and functional features (Fig. 1c, bottom left; see Fig. 6). Collectively, these functions achieve integration across modalities and scales (Fig. 1d-I). For unaligned datasets, the Alignment in the *Filter* provides template-based registration (powered by ANTs) of images and their derived digitized data.

At the output level, BrAVe supports flexible export options ranging from quantitative tables for downstream analysis to static figures and spatiotemporal animations (Fig. 1a-III, and Fig. 1d-V). A client-server architecture (Fig. 1a-IV) ensures scalability and

high-performance visualization and analysis of large-scale datasets (Fig. 1d-III). All visualizations are compatible with immersive exploration in virtual reality (VR) for enhanced spatial perception and interaction (Fig. 1d-VI). Together, these features make the platform both intuitive and practical.

In sum, BrAVe supports an end-to-end workflow from multimodal data ingestion and spatial registration to quantitative, cross-modal, and spatially resolved integrative analysis, all within a unified, interactive, and scalable 3D environment, without species restrictions (Fig. 1d-VII).

Data handling capability for multimodal atlas datasets across species

To verify that BrAVe provides a unified environment for ingesting and visualizing multimodal brain atlas datasets across species, we curated publicly available resources spanning the three major modalities—molecular (gene expression), structural (neuronal morphology), and functional (whole-brain activity)—from four widely studied model organisms ranging from invertebrates to non-human primates: *Drosophila melanogaster* (fly), *Danio rerio* (zebrafish), *Mus musculus* (mouse), and *Macaca mulatta* (macaque) (Fig. 2). For fly, we adopted the JRC 2018 central brain template[29] (Fig. 2a, left). For zebrafish, we used our nervous system-wide 3D Common Physical Space (CPSv1) as the reference atlas for integrating multimodal datasets[14] (Fig. 2b, left). For mouse and macaque, we adopted the Allen CCFv3[31] (Fig. 2c, left) and the National Institute of Mental Health Macaque Template NMTv2[35] (Fig. 2d, left), respectively.

Molecular datasets, in the form of registered transgenic reporter or *in situ* hybridization images, can be directly loaded into BrAVe and co-visualized with brain structures (Fig. 2a, second column from the left, gene expression images of fly[49]). To enable cell-level visualization, we converted gene expression images into spatial feature point representations, where the 3D coordinates of gene-expressing cells were recorded as individual markers (see Methods). This allows specific gene-labeled cells or transcriptomic cell types to be visualized as color-coded points in 3D. Datasets converted in this way included zebrafish whole-brain hybridization chain reaction (HCR) images[13] (Fig. 2b, second column from the left), mouse MERFISH-based spatial transcriptomics[21] (Fig. 2c, second column from the left), and macaque cortical stereo-seq data[24] (Fig. 2d, second column from the left). Structural datasets consisted of large-scale single-neuron reconstructions had already been registered to their respective templates of the four species[14,19,22,25,50]. These were directly visualized in BrAVe via standardized SWC[51] file format (Fig. 2a-d, middle). Functional activity datasets, such as *in vivo* calcium imaging in fly[52] and zebrafish, or fMRI in mouse[53] and macaque[54], were likewise ingested as volumetric images and registered to the templates for whole-brain visualization (Fig. 2a-d, second column from the right). Across these species, BrAVe thus enables the integrated visualization of molecular, structural, and functional datasets in a common anatomical reference frame (Fig. 2a-d, right; Supplementary Video 1), providing a

foundation for spatial comparison and cross-modal analysis. Detailed metadata, including dataset size, rendering complexity, and source are summarized in Supplementary Table 1.

To benchmark BrAVe performance and scalability, we tested BrAVe using 5,000 neuronal reconstructions from zebrafish and mouse brains, and 2,000 from macaque brains. We quantified five core operations (Extended Data Fig. 1): (1) data reading/parsing (loading SWCs into BrAVe's internal data structure), (2) static rendering (non-interactive 3D visualization), (3) dynamic rendering (real-time interactive visualization), (4) neuronal morphology analysis, and (5) neuron-to-region projection strength analysis. Tests were conducted under two deployment modes (see Methods): a standalone workstation and a two-node GPU cluster (dual A100 GPUs per node). Processing times scaled with the number of points per SWC, such that zebrafish neurons, which contain fewer points, were loaded and analyzed faster than mouse neurons despite equal file counts (Extended Data Fig. 1a,b). The distributed deployment (cluster) significantly accelerated the operations (Extended Data Fig. 1; average time reduction for all five processes: zebrafish, 82 ± 7%; mice, 87 ± 3%; macaque, 60 ± 17%). Under the distributed configuration, reading and rendering thousands of neurons required only several tens of seconds (Extended Data Fig. 1, sum of the first three operations), while computational intensive projection analyses were completed within seconds to about ten minutes.

Together, these results demonstrate that BrAVe robustly supports multimodal brain atlas datasets across species. By leveraging distributed environments, BrAVe enables scalable visualization and analysis, maintaining efficiency even as datasets grow larger and more complex.

Toolkit for neuronal trees: from single-neuron morphology to network wiring

Neurons, as the fundamental units of the nervous system, possess distinct dendritic and axonal compartments that define the directionality of information flow. Their morphology encodes essential clues to both structural and functional connectivity. To characterize and interpret these aspects, BrAVe implements a modular suite of tools, including structural feature extraction, morphological clustering, analysis of dendritic and axonal regional innervation, inference of potential synaptic partners, and topological network exploration and analysis (Fig. 3a).

BrAVe provides customizable visualization and quantitative analysis for single-neuron reconstructions. Users can apply feature-based coloring schemes to distinguish morphological components such as soma, dendrites, and axons (Fig. 3b-i). By integrating core functions of L-measure[55], it enables the extraction of key morphological parameters, including total length, Euclidean distance to soma, and branch number and order. These parameters can be exported in Excel table and rendered directly in 3D—for example, coloring each branch by length or order—thus linking geometric and topological features to spatial context (Fig. 3b-ii,iii). For neuronal populations, BrAVe supports batch loading via a data folder and group-wise

coloring by neuron ID (Fig. 3b-iv), neuronal type (see Methods), individual morphological parameters (such as branch number in Fig. 3b-v), or soma position (Fig. 3b-vi).

Moreover, BrAVe supports neuron clustering based on morphological similarity (Fig. 3c). It includes a built-in implementation of our MBLAST algorithm[14] and allows integration of user-defined clustering methods. Users can flexibly define the number of clusters and thus interactively explore the hierarchical organization through correspondingly rendered dendrogram and cluster-specific neuron visualization (Fig. 3c, bottom). Neuron clusters can be exported and reloaded for customized visualization and wiring analysis (see below).

BrAVe integrates projection analysis with real-time 3D interaction, enabling intuitive exploration of neuron-region relationships. Users can directly right-click neurons or brain regions of interest in the 3D *RenderView* to access a context-sensitive menu and invoke analytical visualizations (Supplementary Video 2). For example, users can select a neuron to query its somatic location, axonal projection regions, and dendritic recipient regions (Fig. 3d, left). Conversely, selecting a region reveals its resident neurons (output neurons) as well as input neurons that project to it, with options for further filtering by the source regions of input neurons (Fig. 3d, middle). In addition, users can define custom groups (e.g., excitatory neurons within a nucleus) (see Methods) and perform neuron-region relationship analyses at the group level. Neuron or neuronal cluster projection strength (axonal length) matrices can be exported as raw tables for downstream analysis or displayed directly in BrAVe as interactive heatmaps with source-target lookup and connectivity strength visualization (Fig. 3d, top right; Supplementary Video 2). The target regions can also be color-coded to directly display projection strength (Fig. 3d, bottom right; Supplementary Video 2). This integration of interactive querying, computation, and visualization, ensures immediate and interpretable readouts.

For neuron datasets annotated with axon-dendrite polarity, BrAVe infers putative synaptic connectivity based on axonal and dendritic spatial proximity within user-defined thresholds (e.g., 2 μm) (Fig. 3e, top; see Methods). This enables reconstruction of microcircuits based on individual neurons or neuronal clusters. As an example, we identified a periventricular projection neuron (PVPN) subtype forming selective connections with retinal ganglion cells (RGCs) targeting the anterior tectal neuropil in zebrafish (Fig. 3e, bottom). Inferred connectivity can be exported (connection matrices and JSON format) or interactively queried in the 3D interface by directly picking specific neurons or neuronal clusters (Fig. 3e, bottom middle and right; Supplementary Video 3). This interactive connectivity query is equally applicable to EM-derived neuronal reconstructions with accurate synaptic connection annotations.

Beyond upstream-downstream circuit exploration, BrAVe supports network-level analysis of neuron-, region-, and any node-based graphs, with or without explicit spatial embedding. Networks can be visualized as abstract node–edge layouts (e.g., random and circular layouts), or as spatially grounded views, where nodes are represented by neuronal

soma or regional centroids, or directly by region or neuron objects themselves (original). BrAVe can also visualize regions arranged by their centroids (radiation), with edges displayed as parabolic arcs (Fig. 3f). Users can specify source-target nodes and path steps to identify all defined communication pathways, which are dynamically linked to 3D network renderings so that selected pathways (including nodes and edges) can be highlighted (Fig. 3g-i,ii). Beyond pathway exploration, BrAVe integrates graph-theoretic analyses to extract higher-order organizational principles. These include motif detection for user-defined node profiles (Fig. 3g-iii) and centrality mapping for highlighting communication hubs and key integrator nodes (Fig. 3g-iv). This network analysis module can be applied to explore diverse types of connectivity networks written as source-target matrices.

Together, these integrated modules transform raw neuron reconstructions into a versatile analytical substrate, enabling multi-scale exploration—from single-cell morphology to circuit to network topology—within a unified spatial framework.

Cross-modal analysis: linking gene expression to neuronal morphology

A central objective of BrAVe is to enable cross-modal integration through spatial correspondence. Structural data are represented primarily by digitized neuronal skeletons (i.e., connected point sets), while molecular and neural activity data are usually expressed as volumetric images, which can be transformed into spatial feature points. Within BrAVe, raw images can be processed using diverse computational operations, most notably Boolean operations (union, intersection, subtraction), to generate derived images that highlight user-defined features of interest. To enable interaction among these diverse modalities, BrAVe implements robust spatial query functions across image-image, image-point, and point-point data types. Leveraging its spatial parsing engine, images or feature points can be mapped onto anatomical regions, and particularly neuronal tracings can be directly queried against these data, thereby generating multimodal annotations at the level of individual objects (Fig. 4a; see Methods).

To demonstrate these functions, we performed cross-modal analyses linking gene expression datasets with neuronal reconstructions. In larval zebrafish, we utilized transgenic labeling for the dopamine D2a receptor *drd2a* and whole-brain hybridization chain reaction (HCR) image for the dopamine D4a receptor *drd4a*[13] (Fig. 4b, I). For each loaded 3D image, BrAVe can render expression intensities (Fig. 4b, II-i) and convert above-threshold expression patterns into spatial feature points, which can be mapped to annotated brain regions (Fig. 4b, II-ii) and allows generation of expression density maps (Fig. 4b, II-iii). By spatially mapping each gene image onto the nervous system-wide single-neuron morphology database[14], we identified the corresponding neuronal populations (Fig. 4b, II-iv; see Methods). By performing HCR-FISH on sparsely labeled fish samples used for single-neuron reconstruction (see Methods), we validated that, among the mapped *drd2a+* and *drd4a+* populations, two reconstructed mitral cells (MCs) with distinct projection patterns were

confirmed to express *drd2a* and *drd4a*, respectively (Fig. 4b, II-v). Boolean intersection of the two images identified areas with overlapping expression of *drd2a* and *drd4a* (Fig. 4b, III-i). These areas were then used to filter the *drd2a+*,*drd4a+* neuronal population, which localized predominantly to the pineal gland (Fig. 4b, III-ii). Consistently, previous studies have also reported the expression of both *drd2a* and *drd4a* in the pineal gland[56,57]. Whole-mount HCR-FISH further revealed the juxtaposed *drd2a+* and *drd4a+* puncta within the pineal gland (Fig. 4b, III-iii), supporting their co-expression in pineal neurons.

In the mouse brain, we analyzed MERFISH-based spatial transcriptomics data[21], which were imported into BrAVe as feature points (see Methods). Spatial distributions of cells expressing four dopamine receptor genes (*Drd1* and *Drd5* representing D1-type receptors, and *Drd2* and *Drd3* representing D2-type receptors) were compared, revealing distinct cell-resolved gene expression abundance (Fig. 4c, I) and regional distribution densities (Fig. 4c, II). Within the hippocampal formation (HPF; Fig. 4d,e), quantitative analysis of cell density across subregions revealed a more enrichment of D1-type receptor-expressing cells compared with D2-type receptor-expressing cells, with *Drd5*-expressing cells showing particularly strong prevalence. This HPF bias contrasted with the whole-brain level, where the densities of D1-type and D2-type receptor-expressing cells were relatively comparable (Fig. 4e, the left bar). By further mapping the positions of gene-expressing cells onto soma locations from hippocampal single-neuron reconstructions[22], BrAVe enables filtering of neurons according to dopamine receptor gene expression (Fig. 4f).

Together, these analyses demonstrate how BrAVe enables the identification of candidate neurons expressing specific genes, thereby facilitating the association of molecular markers with characteristic morphologies. Conversely, it allows searching for molecular markers corresponding to neurons with characteristic morphological features. These capabilities bridge genetic and morphological classification, advancing an integrative multimodal framework for neuronal typing and enabling hypothesis-driven genetic targeting and validation.

Cross-modal analysis: linking neuronal activity to circuit

Through spatial correspondence, BrAVe can integrate functional and structural datasets within a common 3D spatial framework, enabling whole-brain neuronal activity to be mapped onto underlying circuit architectures (Fig. 5a). As a case study, we analyzed whole-brain calcium imaging data recorded from freely swimming larval zebrafish engaged in prey-capture behavior[58]. Neuronal activity dynamics during prey capture were registered to the zebrafish CPSv1 (see Methods) and overlaid with reconstructed single neurons and connectivity datasets[14]. This integration enables frame-by-frame linkage of neuronal activity with morphological reconstructions and brain regions, thereby associating distinct behavioral epochs—including prey detection, J-turn, approach, eye convergence (EC), inhale, swallow, and digestion—with specific morphological ensembles distributed in whole-brain regions (Fig.

5b,c; Supplementary Video 4). Notably, neurons activated during individual epochs displayed both shared and divergent morphologies and projection patterns (Fig. 5c), indicating a combination of continuous transitions and modular recruitment of circuit components across different behavioral stages.

Among activated neurons, we identified contralaterally descending projection neurons in the OTAOS (optic tract and accessory optic system) region of the zebrafish CPSv1 that directly receives RGC inputs (Fig. 5d, I). These neurons belong to the glutamatergic morphotype #Glu-2C0203[14] and exhibited a location and projection pattern identical to the previously reported neuron class that can trigger predatory behavior[59]. We named them pre-capture initiation neurons (PCINs). Using BrAVe's neuronal wiring calculation *Filter*, we traced circuit connections within the activated ensembles, including the sensorimotor partners of PCINs. Morphological matching to ZExplorer excitatory and inhibitory morphotypes[14] revealed diverse neurons involved. During the initial detection epoch, in addition to the visual-related PCIN, we observed activation of olfactory pathways, including olfactory sensory neurons (OSNs) and their downstream MCs in the olfactory bulb (Fig. 5d, II-i). These MCs were further connected to spinal cord-projecting, motor-related neurons in the dopaminergic diencephalic cluster 2 (DC2)[60] (Fig. 5d, II-ii) and to visual-related projection neurons in the optic tectum (OT) via subpallium (Sp) (Fig. 5d, II-iii). These two putative olfactory-relevant circuits require further experimental verification.

During approach and EC epochs, the downstream partners of PCINs included motor coordination-related neurons, such as oculomotor neurons (nIV, the trochlear nerve motor nucleus), reticulospinal neurons (RSNs), and the nucleus of the medial longitudinal fasciculus (nMLF) neurons, relayed via an ascending hindbrain (H) neuron (Fig. 5e, I). Furthermore, we identified long-range ascending neurons downstream of the nMLF and RSNs that projected feedback to multiple sensory regions, including known cholinergic neurons in the octavolateralis efferent nucleus (OEN)[61] projecting to lateral line neuromasts (mechanosensory) (Fig. 5e, II-i), and hindbrain neurons projecting to olfactory bulb (olfactory) (Fig. 5e, II-ii) or tectal neuropil (visual) (Fig. 5e, II-iii). While further experimental validation is required, these candidate feedback pathways highlight potential cross-modal coordination during prey capture.

Altogether, these analyses illustrate that BrAVe enables data-driven discovery of structure-function relationships at cellular resolution across behaviorally relevant circuits. By unifying multimodal datasets—including neuronal activity, morphology, and connectivity—within a common spatial reference, BrAVe provides a platform for *in silico* hypothesis generation.

Cross-scale analysis: integrative LM-EM neuron annotation

Microscale EM datasets often lack definitive cell-type identity, whereas mesoscale LM datasets typically lack true synaptic connectivity. To achieve comprehensive cross-scale

integration, we developed an LM-EM matching function within BrAVe (see Methods). It aligns LM and EM datasets using single-neuronal soma position and morphological similarity, thereby (1) transferring LM-based structural and functional cell-type labels to EM reconstructions, and (2) mapping EM-derived synaptic connectivity onto LM morphotypes.

For EM reconstructions, BrAVe supports joint visualization of EM-derived neuron morphologies and their synaptic connections (Fig. 6a, I), allowing dynamic querying of upstream and downstream partners based on annotated synaptic relationships. For example, by interactively selecting a single postsynaptic site on a locus coeruleus (LC) neuron, an individual presynaptic neuron can be retrieved and visualized (Fig. 6a, II). To infer the cell-type identity of this upstream partner, we performed morphology-based matching against LM reconstructions in the ZExplorer single-neuron atlas[14]. This analysis revealed three neurons in close proximity with high similarity scores, all belonging to the glutamatergic morphotype #Glu-5L0701[14] (Fig. 6b). Neurons of this morphotype correspond to *vglut2*-positive dopaminergic (DA) neurons in DC6[60,62], suggesting that LC may receive direct DA neuron input.

Conversely, LM neurons can be linked to EM data via morphology-based matching, enabling detailed interrogation of their synaptic connectivity. For example, within the neuronal ensemble that was active during the detection epoch of prey-capture behavior, we identified a neuron whose location and morphology correspond to the spinal cord-projecting A11-type dopaminergic neurons in DC2[60,63] (see Fig. 5d, II-ii). Matching this neuron to EM reconstructions yielded a high-similarity candidate located in DC2 (Fig. 6c, I). This candidate was labeled with cytosolic enhanced ascorbate peroxidase-2, a marker of monoaminergic neurons in the EM data[15], confirming its dopaminergic identity. Further inspection of the EM connectome revealed a presynaptic partner in DC5 (Fig. 6c, II). Based on its soma location and morphology[60], this partner is also likely a dopaminergic neuron, suggesting interconnections between DA nuclei.

This bidirectional LM-EM matching establishes an iterative closed-loop, whereby LM motivates synapse-level EM exploration, and EM-derived connected neurons are mapped back to LM to refine cell-type annotations. Together with the cross-modal analyses (see Figs. 4,5), this integration of LM's cellular-resolution reconstructions with EM's synapse-level details provides a unified framework for cross-scale, cross-modal mapping of neuronal identity, synaptic connectivity as well as neuronal activity.

Discussion

BrAVe addresses a significant challenge in current brain atlas platforms: the lack of a unified and scalable solution for integrative analysis of 3D brain atlas datasets across modalities and scales in diverse species. By abstracting diverse datasets into a set of generalizable data types—volumetric images, parcellated regions, neuronal morphologies, spatial feature points, and connectivity networks—BrAVe accommodates existing brain atlas data, from gene

expression to neuronal morphology to neuronal activity, independent of species. It enables researchers to conduct a continuous analysis workflow, spanning image registration, modality-specific quantification, and cross-modal mapping and integrative interrogation. This capability underpins its importance in providing a foundational solution for integrative deciphering of the molecular, structural, and functional architecture of the brain[28,64].

A key innovation of BrAVe is its capability to support 3D interoperability of multimodal brain data, in accordance with the FAIR guiding principles[65]. By registering diverse datasets into a species-specific anatomical coordinate framework, BrAVe enables dynamic crosstalk between any two modalities based on spatial relationships, for example, mapping gene expression onto neuronal morphologies, mapping brain-wide activity patterns to structural connectivity, or matching LM and EM reconstructions. Ultimately, this framework enables holistic integration of diverse modalities, providing comprehensive multimodal annotations for a single biological entity. In addition, BrAVe couples quantitative analysis and interactive visualization, ensuring that computational results are transparent and intuitively interpretable. Analyses are thus directly anchored to visual evidence, promoting an iterative "see to know, and know to see" cycle of discovery.

Another distinctive feature is accessibility. BrAVe's highly intuitive, GUI-based interface, featuring context-sensitive right-click menu interactions directly within the 3D rendering window, removes barriers for users lacking programming expertise. This contrasts with code-intensive toolkits, significantly broadening application within the neuroscience community. Furthermore, its built-in support for saving, restoring, and recording analysis workflows ensures reproducibility and fosters collaborative development among research teams.

Technically, BrAVe leverages a distributed computing architecture to support high-performance 3D rendering and real-time interaction, even with large-scale datasets such as whole-brain neuronal reconstructions or synaptic connectomes. It also supports algorithmic extensibility, allowing researchers to incorporate custom analytical methods (such as neuronal classification algorithm) while taking advantage of BrAVe's visualization and data mining capabilities. Multiple export options, ranging from structured tables and high-resolution figures to animations and immersive VR content (Supplementary Video 5), along with real-time 3D interactive visualization capabilities, further expand its utility for scientific communication, teaching, and public engagement[66].

Although it was initially developed for neuroscience research, BrAVe's design principles—spatially anchoring of data, standardized formats for common biological modalities, and cross-modal integration—make it applicable across biological systems. Any system in which molecular, structural, and functional datasets can be registered to a common anatomical framework may benefit[67]. For example, BrAVe could be extended to atlas-based investigations of the heart, lung, or kidney, across developmental or pathological states. This

generality positions BrAVe as a versatile spatiotemporal platform for systems biology beyond the brain.

Finally, we envision BrAVe operating within a dual-system ecosystem. The standalone platform (BrAVe) functions as an exploratory engine for cross-modal visual analytics, whereas a web-based interface serves as a data query and structured knowledge portal powered by graph-based ontology[68,69]. Together, they form a mutually reinforcing loop: findings from BrAVe feed into the ontology, while ontology-guided exploration drives targeted analyses within BrAVe. This interplay promotes both hypothesis-driven and data-driven discovery, while supporting open science practices and collaborative exchanges.

In sum, BrAVe provides not only a technical solution but also a conceptual framework for integrative neuroscience. We expect BrAVe to catalyze a paradigm shift in experimental design, in which spatial registration to standardized coordinate systems becomes a guiding principle for data acquisition. Such spatial anchoring not only enhances comparability but also incentivizes harmonization of datasets across laboratories. By unifying multimodal data into a spatially coherent and accessible environment, BrAVe could accelerate the emergence of community-driven, continuously updated atlases that increase in scope and resolution over time, fostering a shared and cumulative scientific resource.

References

1. Zeng, H. & Sanes, J. R. Neuronal cell-type classification: Challenges, opportunities and the path forward. *Nat. Rev. Neurosci.* **18**, 530–546 (2017).
2. Luo, L. Architectures of neuronal circuits. *Science* **373**, (2021).
3. Sultana, O. F., Bandaru, M., Islam, M. A. & Reddy, P. H. Unraveling the complexity of human brain: Structure, function in healthy and disease states. *Ageing Res. Rev.* **100**, 102414 (2024).
4. Zheng, Z. *et al.* A Complete Electron Microscopy Volume of the Brain of Adult Drosophila melanogaster. *Cell* **174**, 730-743.e22 (2018).
5. Cook, S. J. *et al.* Whole-animal connectomes of both Caenorhabditis elegans sexes. *Nature* **571**, 63–71 (2019).
6. Scheffer, L. K. *et al.* A connectome and analysis of the adult Drosophila central brain. *Elife* **9**, 1–74 (2020).
7. Witvliet, D. *et al.* Connectomes across development reveal principles of brain maturation. *Nature* **596**, 257–261 (2021).
8. Winding, M. *et al.* The connectome of an insect brain. *Science* **379**, eadd9330 (2023).
9. Dorkenwald, S. *et al.* Neuronal wiring diagram of an adult brain. *Nature* **634**, 124–138 (2024).
10. Randlett, O. *et al.* Whole-brain activity mapping onto a zebrafish brain atlas. *Nat. Methods* **12**, 1039–1046 (2015).
11. Kunst, M. *et al.* A Cellular-Resolution Atlas of the Larval Zebrafish Brain. *Neuron* **103**, 21-38.e5 (2019).

12. Svara, F. *et al.* Automated synapse-level reconstruction of neural circuits in the larval zebrafish brain. *Nat. Methods* **19**, 1357–1366 (2022).
13. Shainer, I. *et al.* A single-cell resolution gene expression atlas of the larval zebrafish brain. *Sci. Adv.* **9**, 1–10 (2023).
14. Du, X., Yue, Z., Wei, J., Li, W. & Chen, M. Central nervous system atlas of larval zebrafish constructed using the morphology of single excitatory and inhibitory neurons. *bioRxiv* 2025.06.06.658008 (2025).
15. Li, F. *et al.* Multiplexed Neuromodulatory-Type-Annotated EM-Reconstruction of Larval Zebrafish. *bioRxiv* 2025.06.12.659365 (2025).
16. Oh, S. W. *et al.* A mesoscale connectome of the mouse brain. *Nature* **508**, 207–214 (2014).
17. Winnubst, J. *et al.* Reconstruction of 1,000 Projection Neurons Reveals New Cell Types and Organization of Long-Range Connectivity in the Mouse Brain. *Cell* **179**, 268-281.e13 (2019).
18. Peng, H. *et al.* Morphological diversity of single neurons in molecularly defined cell types. *Nature* **598**, 174–181 (2021).
19. Gao, L. *et al.* Single-neuron projectome of mouse prefrontal cortex. *Nat. Neurosci.* **25**, 515–529 (2022).
20. Bulovaite, E. *et al.* A brain atlas of synapse protein lifetime across the mouse lifespan. *Neuron* **110**, 4057-4073.e8 (2022).
21. Yao, Z. *et al.* A high-resolution transcriptomic and spatial atlas of cell types in the whole mouse brain. *Nature* **624**, 317–332 (2023).
22. Qiu, S. *et al.* Whole-brain spatial organization of hippocampal single-neuron projectomes. *Science* **383**, (2024).
23. Schneider-Mizell, C. M. *et al.* Inhibitory specificity from a connectomic census of mouse visual cortex. *Nature* **640**, 448–458 (2025).
24. Chen, A. *et al.* Single-cell spatial transcriptome reveals cell-type organization in the macaque cortex. *Cell* **186**, 3726-3743.e24 (2023).
25. Gou, L. *et al.* Single-neuron projectomes of macaque prefrontal cortex reveal refined axon targeting and arborization. *Cell* **188**, 3806-3822.e24 (2025).
26. Shapson-Coe, A. *et al.* A petavoxel fragment of human cerebral cortex reconstructed at nanoscale resolution. *Science* **384**, eadk4858 (2024).
27. Tyson, A. L. & Margrie, T. W. Mesoscale microscopy and image analysis tools for understanding the brain. *Prog. Biophys. Mol. Biol.* **168**, 81–93 (2022).
28. Leergaard, T. B. & Bjaalie, J. G. Atlas-based data integration for mapping the connections and architecture of the brain. *Science* **378**, 488–492 (2022).
29. Bogovic, J. A. *et al.* An unbiased template of the Drosophila brain and ventral nerve cord. *PLoS One* **15**, 1–24 (2020).
30. Kenney, J. W. *et al.* A 3D adult zebrafish brain atlas (AZBA) for the digital age. *Elife* **10**, 1–20 (2021).
31. Wang, Q. *et al.* The Allen Mouse Brain Common Coordinate Framework: A 3D Reference Atlas. *Cell* **181**, 936-953.e20 (2020).
32. Kronman, F. N. *et al.* Developmental mouse brain common coordinate framework. *Nat. Commun.* **15**, 9072 (2024).

33. Kleven, H. *et al.* Waxholm Space atlas of the rat brain: a 3D atlas supporting data analysis and integration. *Nat. Methods* **20**, 1822–1829 (2023).
34. Tian, X. *et al.* An integrated resource for functional and structural connectivity of the marmoset brain. *Nat. Commun.* **13**, (2022).
35. Seidlitz, J. *et al.* A population MRI brain template and analysis tools for the macaque. *Neuroimage* **170**, 121–131 (2018).
36. Marquart, G. D. *et al.* High-precision registration between zebrafish brain atlases using symmetric diffeomorphic normalization. *Gigascience* **6**, 1–15 (2017).
37. Puchades, M. A., Csucs, G., Ledergerber, D., Leergaard, T. B. & Bjaalie, J. G. Spatial registration of serial microscopic brain images to three-dimensional reference atlases with the QuickNII tool. *PLoS One* **14**, 1–14 (2019).
38. Ni, H. *et al.* A Robust Image Registration Interface for Large Volume Brain Atlas. *Sci. Rep.* **10**, 1–16 (2020).
39. Qu, L. *et al.* Cross-modal coherent registration of whole mouse brains. *Nat. Methods* **19**, 111–118 (2022).
40. Carey, H. *et al.* DeepSlice: rapid fully automatic registration of mouse brain imaging to a volumetric atlas. *Nat. Commun.* **14**, (2023).
41. Erö, C., Gewaltig, M. O., Keller, D. & Markram, H. A cell atlas for the mouse brain. *Front. Neuroinform.* **12**, 1–16 (2018).
42. Court, R. *et al.* Virtual Fly Brain—An interactive atlas of the Drosophila nervous system. *Front. Physiol.* **14**, 1–17 (2023).
43. Feng, L., Zhao, T. & Kim, J. neuTube 1.0: A New Design for Efficient Neuron Reconstruction Software Based on the SWC Format. *eneuro* **2**, ENEURO.0049-14.2014 (2015).
44. Fürth, D. *et al.* An interactive framework for whole-brain maps at cellular resolution. *Nat. Neurosci*. **21**, 895–895 (2018).
45. Bates, A. S. *et al.* The natverse, a versatile toolbox for combining and analysing neuroanatomical data. *Elife* **9**, 1–35 (2020).
46. Claudi, F. *et al.* Visualizing anatomically registered data with brainrender. *Elife* **10**, 1–16 (2021).
47. Blixhavn, C. H. *et al.* The Locare workflow: representing neuroscience data locations as geometric objects in 3D brain atlases. *Front. Neuroinform.* **18**, 1–12 (2024).
48. Ahrens, J., Geveci, B. & Law, C. ParaView: An End-User Tool for Large-Data Visualization. *Visualization Handbook* 717–731 (Elsevier, 2005). doi:10.1016/B978-012387582-2/50038-1
49. Jenett, A. *et al.* A GAL4-Driver Line Resource for Drosophila Neurobiology. *Cell Rep.* **2**, 991–1001 (2012).
50. Chiang, A. S. *et al.* Three-dimensional reconstruction of brain-wide wiring networks in drosophila at single-cell resolution. *Curr. Biol.* **21**, 1–11 (2011).
51. Cannon, R. C., Turner, D. A., Pyapali, G. K. & Wheal, H. V. An on-line archive of reconstructed hippocampal neurons. *J. Neurosci. Methods* **84**, 49–54 (1998).
52. Mann, K., Gallen, C. L. & Clandinin, T. R. Whole-Brain Calcium Imaging Reveals an Intrinsic Functional Network in Drosophila. *Curr. Biol.* **27**, 2389-2396.e4 (2017).

53. Yu, Y. *et al.* Sleep fMRI with simultaneous electrophysiology at 9.4 T in male mice. *Nat. Commun.* **14**, 1–18 (2023).
54. Yao, M. *et al.* High-dimensional topographic organization of visual features in the primate temporal lobe. *Nat. Commun.* **14**, (2023).
55. Scorcioni, R., Polavaram, S. & Ascoli, G. A. L-Measure: a web-accessible tool for the analysis, comparison and search of digital reconstructions of neuronal morphologies. *Nat. Protoc.* **3**, 866–876 (2008).
56. Boehmier, W. *et al.* Evolution and expression of D2 and D3 dopamine receptor genes in zebrafish. *Dev. Dyn.* **230**, 481–493 (2004).
57. Boehmler, W. *et al.* D4 Dopamine receptor genes of zebrafish and effects of the antipsychotic clozapine on larval swimming behaviour. *Genes, Brain Behav.* **6**, 155–166 (2007).
58. Cong, L. *et al.* Rapid whole brain imaging of neural activity in freely behaving larval zebrafish (Danio rerio). *Elife* **6**, 1–20 (2017).
59. Antinucci, P., Folgueira, M. & Bianco, I. H. Pretectal neurons control hunting behaviour. *Elife* **8**, 1–34 (2019).
60. Tay, T. L., Ronneberger, O., Ryu, S., Nitschke, R. & Driever, W. Comprehensive catecholaminergic projectome analysis reveals single-neuron integration of zebrafish ascending and descending dopaminergic systems. *Nat. Commun.* **2**, 112–171 (2011).
61. Odstrcil, I. *et al.* Functional and ultrastructural analysis of reafferent mechanosensation in larval zebrafish. *Curr. Biol.* **32**, 176-189.e5 (2022).
62. Filippi, A., Mueller, T. & Driever, W. vglut2 and gad expression reveal distinct patterns of dual GABAergic versus glutamatergic cotransmitter phenotypes of dopaminergic and noradrenergic neurons in the zebrafish brain. *J. Comp. Neurol.* **522**, 2019–2037 (2014).
63. Haehnel-Taguchi, M. *et al.* Projections of the Diencephalospinal Dopaminergic System to Peripheral Sense Organs in Larval Zebrafish (Danio rerio). *Front. Neuroanat.* **12**, 1–21 (2018).
64. Arkhipov, A. *et al.* Integrating multimodal data to understand cortical circuit architecture and function. *Nat. Neurosci.* **28**, 717–730 (2025).
65. Wilkinson, M. D. *et al.* The FAIR Guiding Principles for scientific data management and stewardship. *Sci. Data* **3**, 160018 (2016).
66. Evagorou, M., Erduran, S. & Mäntylä, T. The role of visual representations in scientific practices: from conceptual understanding and knowledge generation to ‘seeing’ how science works. *Int. J. STEM Educ.* **2**, 1–13 (2015).
67. Börner, K. *et al.* Anatomical structures, cell types and biomarkers of the Human Reference Atlas. *Nat. Cell Biol.* **23**, 1117–1128 (2021).
68. Kleven, H. *et al.* AtOM, an ontology model to standardize use of brain atlases in tools, workflows, and data infrastructures. *Sci. Data* **10**, 486 (2023).
69. Herr, B. W. *et al.* Specimen, biological structure, and spatial ontologies in support of a Human Reference Atlas. *Sci. Data* **10**, 171 (2023).

Methods

BrAVe layout

Upon startup, BrAVe presents an initialization interface promoting users to select a species-specific reference brain, which establishes the coordinate framework for subsequent analyses. Users can also define the operating mode as either visualization-only or visualization-and-analysis. Once launched, BrAVe displays a modular interface comprising seven core components:

1. Menu Bar – Provides essential functionalities, including data import/export, 3D view configurations, volumetric data cropping and slicing, custom viewpoint management, animation playback, and access to the *Filter* toolbar. The *Filter* toolbar enables one-click access to built-in analytical modules, such as morphological quantification, neuronal wiring calculation, and network connectivity analysis.
2. Pipeline Browser – Organizes all imported datasets and analytical outputs hierarchically, allowing users to track and manage data processing workflows.
3. Data Browser – Lists all loaded neuronal tracings, brain regions, image volumes, and feature points in structured modules. It supports searching, sorting, toggling visibility, customizing colors, and interactive highlighting.
4. Properties Panel – Enables parameter adjustment for items in the processing pipeline, such as color, opacity, rendering settings, and analytical thresholds.
5. 3D RenderView – Serves as the central environment for interactive 3D visualization, facilitating real-time exploration of multimodal brain data and derived analytical results.
6. Context-Sensitive Right-Click Menu – Offers shortcut operations within the RenderView, including toggling visibility of all or specific data types, switching color-coding schemes of neuronal tracings, executing group-based operations (see the section "Group function" in Methods), exploring neuron-region relationships and inter-neuronal connectivity, and exporting projection or connectivity matrices.
7. Animation View – Allows users to define camera trajectories, control display sequences, and adjust rendering settings to generate customized animations of multimodal brain data.

Basic tutorials

We illustrate BrAVe's workflow using neuron-centric visualization and analysis as an example, demonstrated with the zebrafish CPSv1 reference atlas:

1. Launching software and selecting reference atlas

   Select "Zebrafish CPSv1" in the startup interface and click "Start".
2. Loading multimodal data

   Click "Open" to import datasets. In the dialog box, select folders containing neuronal tracings and brain regions. Assign appropriate readers (e.g. Neuronal Tracing Data Folder Reader or Region Data Folder Reader) and click "Apply".
3. Visualizing data and controlling visibility

Toggle dataset visibility using the eye icons in the Pipeline Browser or Data Browser. Within the RenderView, right-click to open the context menu and select “Show Only Neuronal Type” → [specific type] to isolate neurons by type (see the section “Neuronal type annotation” in Methods), or “Show Only Neural Structure” → “Soma/Axon/Dendrite” to display specific compartments.

4. Analyzing neuronal morphology

   Select a neuronal tracing data in the Pipeline Browser, click the “Neuronal Morphology” *Filter* icon in the *Manu Bar*, select the analysis target (entire neuron, axon, or dendrite) in the *Properties Panel*, and designate an output directory. Click “Apply” to run the analysis, and results are exported as Excel spreadsheets.

5. Exploring neuron-region relationships

   Right-click a neuron to open the context menu and select “Show Only Neuron” → [regions with specified relationship] to isolate the neuron alongside its soma-locating, dendrite-innervating, or axon-projecting regions. Conversely, right-clicking a brain region and selecting “Show Only Region” → [neurons with specified relationship] retrieves neurons associated with that region.

6. Exporting projection metrics

   Within the *RenderView*, right-click to open the context menu and navigate to “Analysis And Export” → “Projection Weight” → “Neuron-Region” → [specific projection metric]. Specify a save location; results are exported as structured Excel files for downstream analyses.

7. Managing sessions

   Save or restore sessions via “File” → “Save State...” and “File” → “Load State...” for continuity or reproducibility.

Neuronal type annotation

BrAVe supports visualization and analysis of imported neuronal tracing data by user-defined neuronal types, organized in a two-tier hierarchy (main type and subtype). Type-based operations, such as toggling visibility and assigning colors, can be quickly accessed via the context menu or “Data Browser”. Projection-related analyses, including projection heatmap visualization and projection weight matrix export, can be automatically executed for each neuronal type.

Two annotation methods are supported: (1) Filename-based annotation, where the subtype name is included in the filename, prefixed by an underscore (“_”), and mapped to a main type in the source code (e.g. subType2MainTypeMap[“vglut2a”] = “Excitatory”); and (2)

JSON-based annotation, where hierarchical type information is embedded directly in the neuron JSON file (see the section "JSON file applications" in Methods). When detected, type information is shown in the context menu and displayed via tooltips upon hover.

Group function

BrAVe enables selective management of subsets of imported data through a "Group" function, supporting targeted visualization and analysis of multimodal elements such as neurons, brain regions, and feature points. Groups can be defined through two methods: (1) Box selection, activated via the context menu item "Select into Group", enabling rectangular region selection on screen; and (2) Pick selection, allowing users to right-click individual elements, view metadata, and add/remove them from groups via "Add into/Remove from Group" → "Picked" menu items. Group states can be saved/loaded via "Save/Load Group State" menu items for reproducible workflows.

Grouped data can be manipulated like general data, including exporting basic information, toggling visibility, adjusting global rendering settings (e.g., color, opacity), and exploring neuron-region relationship and neuronal connectivity. BrAVe also provides a dedicated panel for creating and managing multiple groups, enabling combinatorial visualization and comparative analysis within a single RenderView.

Neuronal wiring analysis based on morphology

Neuronal connectivity was inferred using the Neuronal Wiring Calculation *Filter*, which evaluates axodendritic spatial proximity in single-neuron reconstructions. Four computational models were implemented: center, cubic, cylinder, and tube. The first three assess the local proximity of individual neurite compartments, while the tube model evaluates entire axonal or dendritic volumes. Users can define proximity thresholds based on model radii (see Fig. 3e, top) and further filter connectivity using either the number of qualified compartment pairs (center model) or volumetric overlap (absolute or relative; cubic, cylinder, and tube models). Analyses can be refined by restricting branch types, such as fork-fork or fork-terminal branches. The resulting directed and weighted connectivity networks can be exported, with nodes representing individual neurons or neuronal clusters and edge weights defined by either compartment pair counts or overlapping volume.

Cross-modal mapping based on spatial queries

To enable cross-modal mapping, BrAVe provides a spatial data filtering framework that links data with structural, molecular, or functional features. Take neuron filtering as an example, filtering can be performed based on images or feature points. In the image-based mode, soma positions are evaluated against volumetric images (e.g., immunohistochemistry, calcium imaging), and neurons are retained if the corresponding voxel intensity falls within a user-defined range. In the feature point-based mode, Euclidean distances between neuron somata and feature points (e.g., gene-expressing cells, multi-unit recording sites) are

calculated, and neurons are retained if they lie within a user-defined proximity threshold, optionally constrained by feature-specific scalar values (e.g. gene expression level, neural activity strength). The output includes the resulting neuron subsets and a point cloud of the qualifying image voxel locations or spatial features points for subsequent visualization and quantitative analysis.

LM-EM matching based on morphological similarity

To enable correspondence between LM and EM reconstructions, BrAVe provides a Neuron Similarity *Filter*. Neurons are represented as SWC point clouds, and pairwise similarity is computed using distance-based metrics, including Chamfer (the bidirectional average closest point distance), directed Chamfer (forward and reverse), centroid Euclidean, and Hausdorff distances. Distances are converted to similarity scores as inverse functions of (1 + distance). To improve efficiency, candidate pairs are first pre-filtered by soma proximity (user-defined SomaDistanceThreshold), followed by fast nearest-neighbor searches using k-d trees and parallel processing of neuron pairs. For each neuron, similarity scores are ranked, and only the top N partners (specified by Neuron Count in the *Properties Panel*) above a user-defined similarity threshold are retained. Comparisons can be restricted within or between neuronal clusters (ClusterRelation). The output provides ranked similarity lists for each neuron, which can be exported in CSV/JSON formats or directly visualized in BrAVe, thereby enabling systematic matching of LM morphotypes with EM-derived reconstructions.

JSON file applications

BrAVe employs JSON (JavaScript Object Notation) files to store metadata for multimodal datasets. Metadata is organized through predefined keywords written as associative arrays in JSON format. Each dataset entry is indexed by a datum ID, which acts as a unique identifier linking to the value lists of various relationship-specific keywords. For example, in a neuron JSON file, the keywords “type_array”, “output_region_array”, and “upstream_neuron_array” specify the hierarchical neuronal type, IDs of target projection regions, and IDs of potential input neurons (see the section “Neuronal wiring analysis based on morphology” in Methods), respectively.

Users can create JSON files manually or export them directly from BrAVe after data processing. To export, right-click in the RenderView layout to open the context menu, and navigate to “Analysis and Export” → “General Information” → “All in Separate/Single JSON file”. To apply JSON files, place them in the corresponding data folder and name them info.json. When loading data, BrAVe automatically detects info.json and prioritizes it as the source of input metadata. This eliminates redundant computation, which is particularly beneficial for resource-intensive tasks such as neuron projection analysis and neuronal/synaptic wiring analysis in large-scale datasets.

User manual

Comprehensive documentation, including video- and text-based tutorials, detailed algorithmic descriptions, and developer resources, is available at: https://zebrafish.cn/BrAVe.

Performance benchmarking

We benchmarked BrAVe in standalone and client-server modes. Standalone tests were conducted on a DELL Precision T7920 Tower workstation (Intel® Xeon® Gold 6250 CPU, 3.90 GHz; 768 GB RAM; dual 1.86 TB NVMe SSDs; NVIDIA GeForce RTX 3060 GPU, 12 GB). Client-server tests used the same workstation as the client and a high-performance computing (HPC) cluster as the server, coordinated by SLURM. HPC nodes were configured with dual AMD EPYC 7742 64-core processors (2.30 GHz) and dual NVIDIA A100 GPUs (40 GB each), connected to the storage system via InfiniBand. Server instances were launched with MPI using mpirun -np 4 pvserver.

Three neuron reconstruction datasets were tested: (i) 5,000 zebrafish neurons (264 MB; 14,153,576 nodes), (ii) 5,000 mouse neurons (12,000 MB; 458,603,220 nodes), and (iii) 2,000 macaque neurons (887 MB; 30,547,138 nodes). Prior to each test, the system was reinitialized to ensure consistent runtime environments. Each test was repeated six times under both deployment modes, with execution log files captured (`-l=log.txt,9`) to record runtimes. Execution times (in seconds) were extracted from log files for performance evaluation.

Preprocessing of spatial transcriptomics data of mice and macaque

MERFISH data (MERFISH-C57BL6J-638850) from an adult C57BL/6J mouse brain were obtained from the Allen Brain Atlas (https://alleninstitute.github.io/abc_atlas_access/descriptions/WMB_dataset.html). For Fig. 2, cell coordinates pre-mapped to the Common Coordinate Framework (CCFv3) were integrated with cell-type annotations. One single output file (columns: cell-type identifier, *x*, *y*, *z*) was generated for BrAVe visualization. For Fig. 4, raw gene counts were processed in R (v4.2.2) with Seurat (v5.0.1), normalized with SCTransform using variance-stabilizing transformation (clip range [–10, 10]), and integrated with cell coordinates. For each gene, final outputs (columns: cell-type identifier, *x*, *y*, *z*, normalized gene expression) were exported for BrAVe visualization and analysis. Stero-seq data from macaque brain slices ("macaque1") were obtained from https://macaque.digital-brain.cn. Cell coordinates and cell-type annotations were processed analogously.

Digitization of zebrafish gene expression atlas

The mapzebrain volumetric image atlas of cellular-resolution gene expression[13] was registered to the zebrafish CPSv1 using an inter-atlas transformation[14]. Cell positions (soma centroids) expressing specific genes were manually annotated in Fiji using the Cell Counter plugin and then transformed to the CPS using `antsApplyTransformsToPoints` in the

Advanced Normalization Tools (ANTs)[70]. For each gene, a feature-point CSV file containing cell coordinates was generated for BrAVe visualization and analysis.

Zebrafish husbandry and preparation

Adult zebrafish were maintained at 28 ℃ in an automatic housing system at the National Zebrafish Resources of China (Shanghai, China). Experimental larvae were raised in 10% Hanks' solution containing (in mM): 140 NaCl, 5.4 KCl, 0.25 Na_2HPO_4, 0.44 KH_2PO_4, 1.3 $CaCl_2$, 1.0 $MgSO_4$ and 4.2 $NaHCO_3$ (pH 7.2) under a 14 h:10h light:dark cycle at 28 ℃. Larvae sparsely labeled with tdTomato in neurons at 6 days post-fertilization (dpf), used for multiplexed fluorescent *in situ* hybridization (FISH), were derived from preserved samples previously prepared for single-neuron morphology acquisition[14]. All animal procedures were approved by the Animal Care and Use Committee of the Center for Excellence in Brain Science and Intelligence Technology, Chinese Academy of Sciences (NA-046-2023).

Multiplexed hybridization chain reaction-fluorescence *in situ* hybridization (HCR-FISH)

Larvae with sparsely tdTomato-labeled neurons were fixed in 4% paraformaldehyde (PFA) at 4 °C for 24 h, washed twice with 1× phosphate-buffered saline (PBS), and transferred to 100% methanol at 4 °C for long-term storage. Prior to hybridization, samples were rehydrated by two 10-min washes in 2× saline–sodium citrate (SSC) buffer at room temperature and photobleached overnight at 4 ℃ using an 18 W white LED to minimize tissue autofluorescence.

HCR-FISH was performed following a modified protocol[71]. Briefly, samples were post-fixed, permeabilized, and digested with proteinase K before hybridization with custom-designed DNA probes (synthesized by Beijing Tsingke BioTech) targeting *drd2a* (ID: SHP25061100009), *drd4a* (ID: SHP25061100010), and *tdTomato* (ID: SHP25011000003). After stringent washes, signal amplification was achieved using snap-cooled fluorescent hairpins conjugated to Alexa Fluor 488, Alexa Fluor 546, or JF-669 (synthesized by Sangon Biotech) in amplification buffer (Molecular Instruments). Excess hairpins were removed with a 5× SSCT wash, and samples were stored at 4 ℃ in the dark until imaging.

Confocal imaging

Samples were embedded in 2% low-melting-point agarose in 1× PBS and imaged with an Olympus FV3000 upright confocal microscope with a 20× water-immersion objective (N.A. 1.0). *Z*-stacks were acquired in the upward direction at a voxel resolution of ~ 0.49 × 0.49 × 2.5 μm. To compensate for fluorescence attenuation, laser power was progressively increased

along the *z*-axis. Excitation wavelengths were 488 nm, 561 nm, and 640 nm for Alexa Fluor 488, Alexa Fluor 546, and JF-669, respectively.

Zebrafish prey capture behavior

Transgenic larvae *Tg(elavl3:H2B-GCaMP6f)jf7*[72] expressing a pan-neuronal calcium indicator in a *nacre* background, were used for behavioral imaging. Larvae were raised at 28 °C and imaged at 6 dpf. To enhance prey-capture motivation, individual larvae were food-deprived for 12 h before recording. Each larva was placed in a custom imaging chamber (45 mm diameter, 0.8 mm depth) containing 10% Hanks' solution and ~200 paramecia as prey. The chamber was covered with a 1 mm-thick coverslip to ensure a stable imaging environment.

3D tracking for whole-brain neuronal Ca^{2+} imaging in freely swimming zebrafish

Real-time 3D tracking was implemented similarly to a previous demonstration[58] to enable stable whole-brain calcium imaging in freely swimming larvae. Briefly, larvae were illuminated with near-infrared (NIR) LEDs, and a high-speed camera (Basler ace acA1920-155μm; 1.5 ms exposure, 167 fps) captured scattered light for in-plane tracking. A custom LabVIEW program extracted fish centroid and orientation from each frame and a control algorithm drove a two-axis direct-drive stage (Shanghai YIDING DDHD-4D54D5AP) to compensate for in-plane movement.

Axial (*z*-axis) tracking was achieved by a custom detector comprising a microlens array conjugated to the back pupil of the imaging objective and a camera (Basler aca2000–340km NIR; 90 fps) positioned at its focal plane. Depth was estimated by computing distance variations between images from individual microlenses. The positional error between the fish head and the set point was fed into a proportional-integral-derivative controller, which actuated a pair of piezoelectric stages (Harbin Core Tomorrow Science & Technology, P06.X500R) to stabilize axial position.

Registration of brain Ca^{2+} imaging data from freely moving zebrafish

For each fish, a reference brain was generated from a single 3D whole-brain imaging volume (600 × 600 × 250 voxels) with minimal motion artifacts. Principal axes were computed by covariance matrix analysis, and affine transformations were applied to standardize brain orientation and scale (resampled to 240 × 500 × 170 voxels). Other volumes were aligned to this reference via covariance-based axis alignment, cross-correlation-based translation optimization, and iterative refinement of rotation angles using maximum-intensity projections. Finally, aligned brain stacks of individual fish were registered to the zebrafish CPSv1 using ANTs[14].

Calcium imaging data analysis

Calcium imaging data were processed using a custom script to compute fluorescence changes ($\Delta F/F_0$). A brain mask was first applied to exclude non-brain regions. The baseline

fluorescence (F_0) was defined as the average intensity of six baseline frames acquired prior to the onset of prey capture behavior. For each frame, $\Delta F/F_0$ was calculated as $(F-F_0)/F_0$, scaled by a factor of 20 to enhance visual contrast, and converted to 8-bit format. The processed data were exported as multi-page TIFF files for direct import into BrAVe.

Reporting summary

Further information on research design is available in the Nature Port-folio Reporting Summary linked to this article.

Data availability

Datasets used in this study are publicly available: (1) *Drosophila* – brain template[29], gene expression images[49], and neuronal tracings[50] from http://www.virtualflybrain.org; brain activity (calcium imaging)[52] from https://data.mendeley.com/datasets/8b6nw2xxhn/1. (2) Zebrafish – brain template and LM single-neuron morphology atlas[14] from https://zebrafish.cn/LM-Atlas/EI; gene expression atlas[13] from https://mapzebrain.org; EM reconstructions[15] from https://ng.zebrafish.digital-brain.cn/Fish-X/Manual_supervoxels; whole-brain activity (calcium imaging) from this paper (a doi is available as of the publication date); (3) Mouse – brain template (Allen CCFv3)[31] from http://atlas.brain-map.org; spatial transcriptomic atlas[21] from https://knowledge.brain-map.org/abcatlas; single-neuron morphology atlas[19,22] from https://mouse.braindatacenter.cn; brain activity (fMRI)[53] from https://doi.org/10.12412/BSDC.1668502646.20001. (4) Macaque – brain template (NMTv2)[35] from https://afni.nimh.nih.gov; spatial transcriptomics data[24] from https://macaque.digital-brain.cn/spatial-omics; single-neuron morphology atlas[25] from https://zenodo.org/records/15128612; brain activity (fMRI)[54] from https://doi.org/10.12412/BSDC.1685411291.30001.

Code availability

BrAVe (built on Paraview 5.12.0) is fully open source. All source code and software packages are available at https://github.com/soaringdu/Proj-BrAVe as of the publication date.

References (Methods)

70. Avants, B. B. *et al.* A reproducible evaluation of ANTs similarity metric performance in brain image registration. *Neuroimage* **54**, 2033–2044 (2011).
71. Li, J. *et al.* Neural-activity-regulated and glia-mediated control of brain lymphatic development. *Cell* **188**, 3274-3290.e16 (2025).
72. Dunn, T. W. *et al.* Brain-wide mapping of neural activity controlling zebrafish exploratory locomotion. *Elife* **5**, 1–29 (2016).

Acknowledgments

We are grateful to Dr. Chun Xu, Yu Mu, Shengjin Xu, and Tielin Zhang from the advisory committee of the institutional Center for Data and Computing in Brain Science; Tingting Zhao from the Zebrafish Group of the institutional research facility for Mapping Brain-Wide Mesoscale Connectome; and Jun Zhang from Achievement Transformation Office for their support in the implementation and documentation of BrAVe. We thank Tianlun Chen, Qimeng Zhao, Meiyu Zheng, Xin Wang, Hongli Wan, and Tingting Zhao for their assistance with software tutorials. We thank Hao Yang from Dr. Zhifeng Liang's laboratory for assistance with macaque transcriptomic data processing, Dr. Chao Li for assistance with HCR-FISH experiments, and Shan Wang for help with VR-related video recording. This work was supported by STI2030-Major Projects (2021ZD0204500, 2021ZD0204502, 2021ZD0204504, and 2022ZD0209600), the National Natural Science Foundation of China (32321003, 62320106010, 3240071028, 62276253, and U22B200571), Shanghai Municipal Science and Technology Major Project (18JC1410100 and 2018SHZDZX05), and Key Research Program of Frontier Sciences (QYZDYSSW-SMC028) and Strategic Priority Research Program (XDB32010200) of Chinese Academy of Sciences. X.F.D. is also supported by the Youth Innovation Promotion Association, Chinese Academy of Sciences.

Author contributions

X.F.D. and J.L.D. conceived and supervised the study. Z.F.Y. selected the ParaView infrastructure. X.F.D., J.L.D., and Y.F.W. designed the overall framework. J.F.W. developed the software with input from H.B.M., with Y.W.Z. contributing to quality control. M.Q.C., H.B.M., J.F.W., Y.W.Z., S.X.C., and J.Q.G. prepared the software tutorials with input from X.F.D. and Y.F.W.. C.X.J. designed the software logo, boot animation, and icons. F.N.L. provided the EM data. T.L.Z acquired brain functional imaging data from freely moving zebrafish during prey capture behavior, under the supervision of K.W.. C.C. and Y.F.W. conducted HCR-FISH experiments under the supervision of S.J.X.. X.D.Z performed confocal imaging. Y.M.Z. processed the spatial transcriptomics data. Y.F.W. and M.Q.C. analyzed the data and prepared illustrations with input from H.B.M. and X.F.D.. Y.F.W. and M.Q.C. generated the videos. X.F.D. and J.L.D. wrote the manuscript with input from all authors.

Competing interests

The authors declare no competing interests.

Figures and Legends

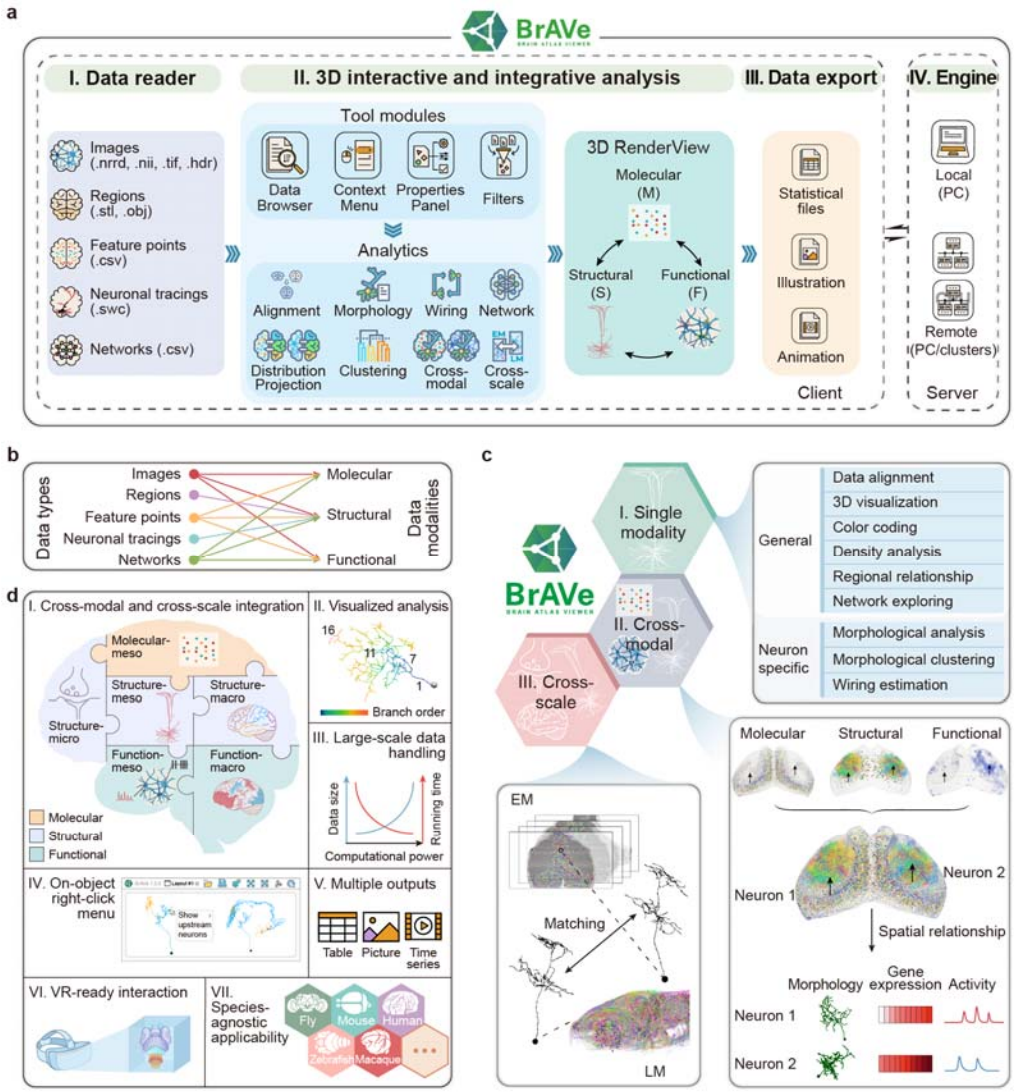

Fig. 1 | Overview of BrAVe: system architecture, core functions and key features.

a, System architecture and workflow. BrAVe comprises a client interface (I–III) and a server engine (IV) that can run locally or on a remote high-performance cluster. The client manages multimodal data import (I, purple), processes it through four tool modules with multiple analytic functions (II, blue), and performs single-modality and multimodal integrative analyses in an interactive 3D viewer (II, teal). Results can be exported as tables, pictures, or videos (III, orange).

b, Correspondence between supported data types (left) and data modalities (right).

c, Core functions. (I) Single-modality analysis (top-right), offering both general and modality-specific tools. (II) Cross-modal integrative analysis (bottom-right), enabling spatial mapping of molecular, structural, and functional data at cellular resolution to assign multimodal annotations to individual neurons. Arrows mark the soma position of two representative neurons. (III) Cross-scale matching (bottom-left), allowing bidirectional correspondence between electron microscopy (EM) and light microscopy (LM)

reconstructions.

d, Key features. (I) Integration of multimodal datasets across scales. Background colors denote data modalities. (II) Visualization of quantitative analyses, for example by coloring neuronal morphology according to branch order. Numbers indicate the order of four representative branches. (III) Large-scale data handling. The schematic shows that, as computational power increases, data size (blue) increases while running time (red) decreases. (IV) Interactive 3D object-based queries via a context menu. For example, right-clicking on an optic tectum neuron (left) allows retrieve of its presynaptic retinal ganglion cells (right). Soma, black; dendrite, yellow; axon, cyan. (V) Flexible export of results, including tables, pictures, and videos. (VI) Immersive data exploration in virtual reality (VR). (VII) Species-agnostic compatibility, supporting brain atlases of fly, zebrafish, mouse, macaque, human, and other model organisms.

See also Supplementary Videos 1 and 5.

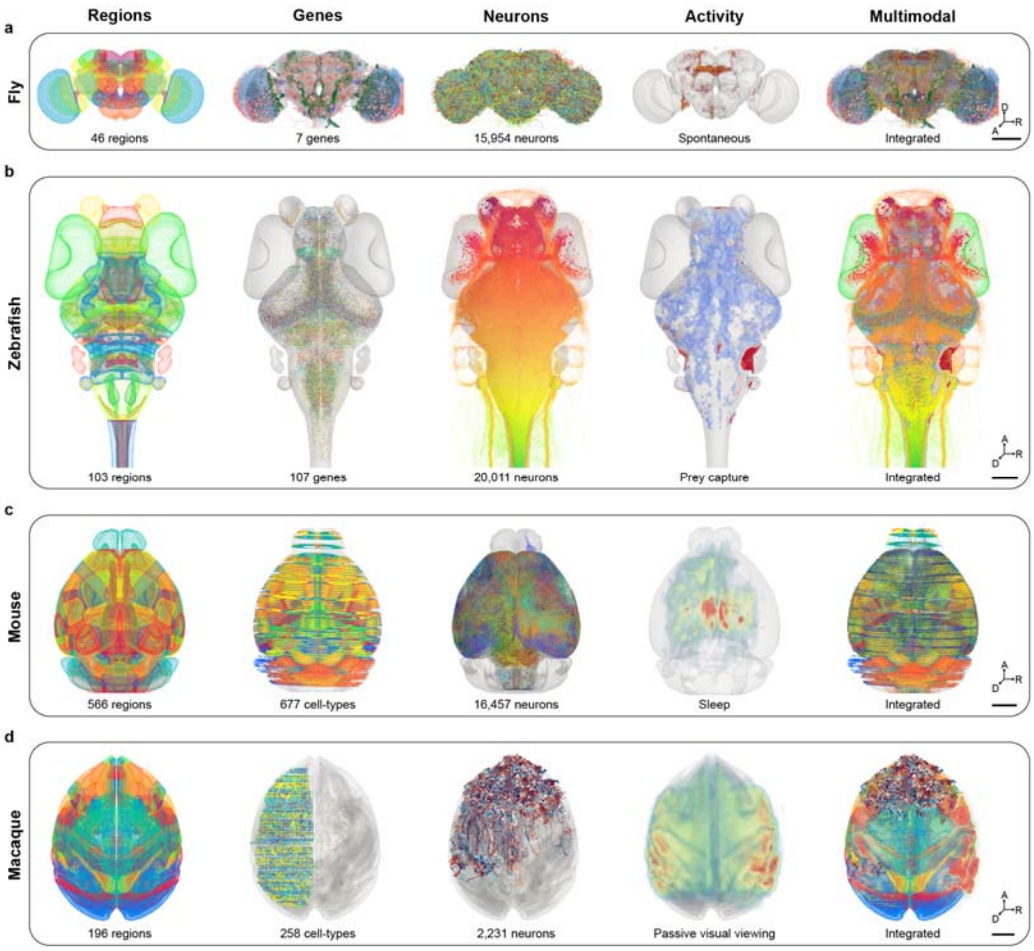

Fig. 2 | Co-visualization of multimodal data in 3D reference atlas across species.
Left to right: anatomical regions, spatial gene expression, neuronal tracings, functional activity maps, and multimodal overlay for fly (**a**), zebrafish (**b**), mouse (**c**), and macaque (**d**).
a, Fly brain reference atlas (JRC 2018) with 46 regions[29], 7 gene-expression images[49], and 15,954 neuronal tracings[50], color-coded by identity; brain-wide spontaneous neuronal calcium activity[52], color-coded by fluorescence intensity; integrated cross-modal visualization of gene expression, neuronal tracing, and neuronal activity datasets.
b, Zebrafish brain reference atlas (ZExplorer CPSv1.0) with 103 regions[14], 107 gene-expression maps[13], and 20,011 neuronal tracings[14], color-coded by identity; brain-wide neuronal calcium activity during the approach & eye convergence epoch of prey-capture behavior (see Fig. 5), color-coded by $\triangle F/F_0$; integrated cross-modal visualization of gene expression, neuronal tracing, and neuronal activity datasets.
c, Mouse brain reference atlas (Allen CCFv3) with 566 regions[31], 677 cell-types inferred from spatial transcriptomics[21], and 16,457 neuronal tracings (6,357 from prefrontal cortex[19] and 10,100 from hippocampus[22]), color coded by identity; fMRI activity during sleep[53], color-coded by image intensity; integrated cross-modal visualization of gene expression, neuronal tracing, and fMRI activity datasets.
d, Macaque brain reference atlas (NMTv2) with 196 regions[35], 258 cell-types inferred from

spatial transcriptomics[24], and 2,231 neuronal tracings[25], color coded by identity; fMRI activity during passive visual viewing[54], color-coded by image intensity; integrated cross-modal visualization of gene expression, neuronal tracing, and fMRI activity datasets.

Scale bars: 100 μm (**a**,**b**), 2 mm (**c**), 10 mm (**d**). A, anterior; D, dorsal; R, right.

See also Supplementary Tables 1 and 2, Supplementary Video 1, and Extended Data Fig. 1.

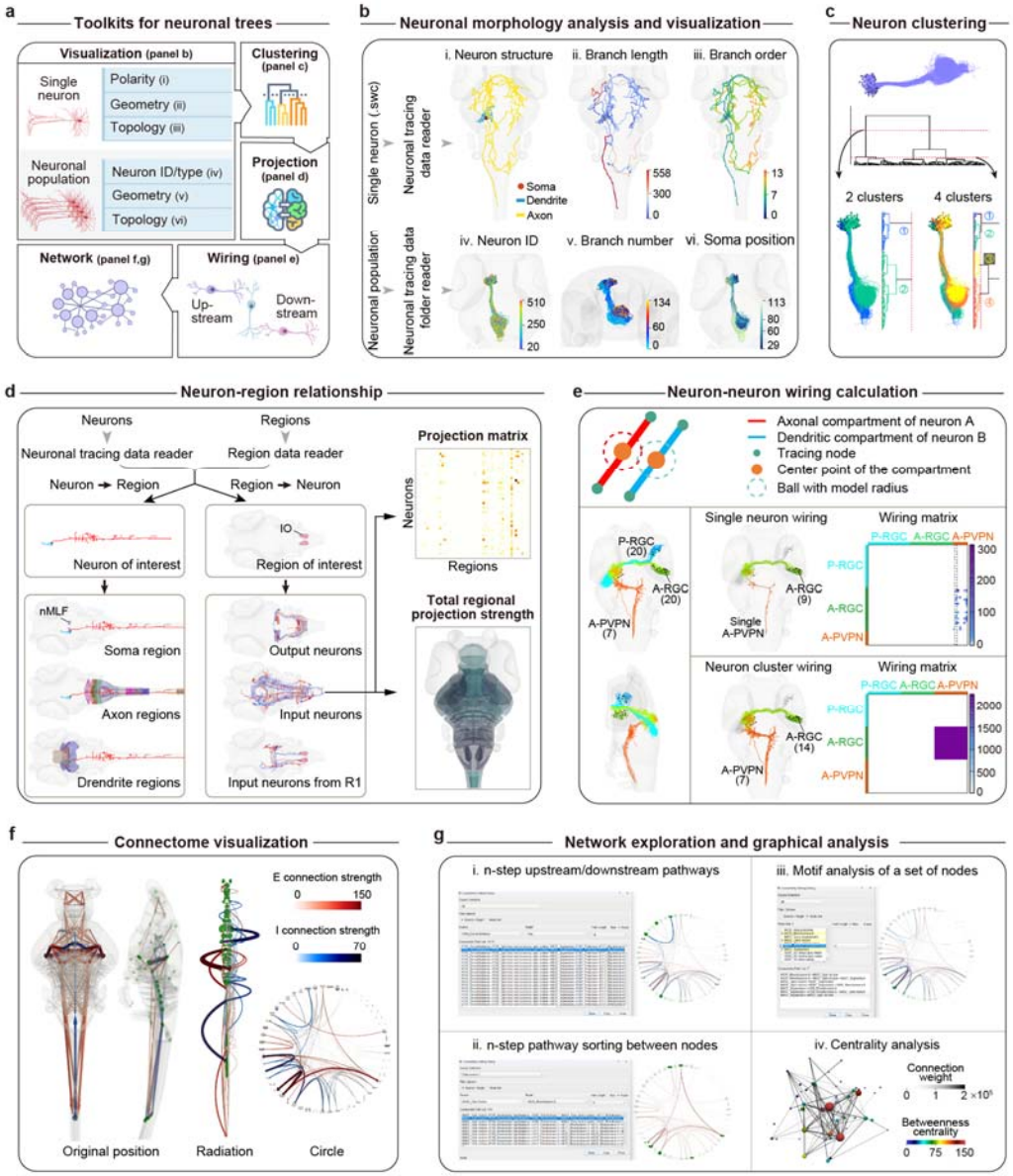

Fig. 3 | Analytical toolkits for neuronal structures.

a, Toolkits for neuronal structure analysis comprising modules for visualization, clustering, projection mapping, wiring calculation, and network analysis.

b, Neuronal morphology analysis and visualization. Top: single-neuron renderings color-coded by morphological components (i), branch length (ii), or branch order (iii). Bottom: population-level visualizations with neurons color-coded by identity (iv), branch number (v), or somatic position (vi).

c, Interactive clustering of neuronal populations. Input neurons (top) with dendrogram (middle) cut at two levels (red dashed lines), yielding either two clusters (bottom left) or four clusters (bottom right). Neurons and dendrogram branches are color-coded by cluster identity.

d, Neuron-region relationship exploration. Left (neuron-to-region query): an nMLF neuron showing soma location, axonal projection targets, and dendritic innervation regions. Middle (region-to-neuron query): neurons located in (output), projecting to (input), or projecting to

the IO from a specific region (R1). Right (projection strength analysis): single-neuron projection matrix (top) and regional projection map (bottom, color-coded by total projection strength) of IO input neurons. Projection strength is calculated as total axonal length terminating in each region.

e, Neuron-neuron wiring analysis. Top: schematic of the 'center' computational mode for inferring connectivity by axodendritic spatial proximity (see Methods). Bottom left: RGCs targeting anterior (green) or posterior (blue) optic tectal neuropil (A-RGCs and P-RGCs), and a PVPN subtype (orange, A-PVPN) included in analysis. Bottom right: circuit rendering (left, with all RGCs and PVPNs shown in grey as background) and wiring matrices (right) at single-neuron (top) and cluster (bottom) levels. Connection strength is quantified as the number of axon–dendrite compartment pairs within a 1-μm radius. The area between the two dashed lines marks the upstream RGC connectivity to the single PVPN. Numbers in brackets indicate the number of neurons visualized.

f, Connectome visualization. Zebrafish interregional excitatory (red) and inhibitory (blue) connectomes[14] rendered in multiple layouts: 3D anatomical (without or with region-centroid spheres, left), radial (regions arranged by *y*-axis position, middle), and circular (regions arranged in a ring, right). Connection strength is encoded by edge color and width, and additionally by parabola height in the radial layout.

g, Network analysis toolkit. Left: network exploration of the connectome in (**f**), including (i) six-step downstream pathways from dorsal thalamus and (ii) six-step paths between the OT and R8. Right: graph-theoretic analyses, including (iii) motif detection within selected node sets (R8, OT, and tegmentum) and (iv) centrality analysis, with nodes arranged in a random layout and color-coded by betweenness centrality, and edges color-coded by connection weight. For i–iii, the selected pathways highlighted in a circular layout (right).

IO, inferior olive; nMLF, nucleus of the medial longitudinal fasciculus; OT, optic tectum; PVPN, periventricular projection neuron; R1/8, rhombomere 1/8; RGC, retinal ganglion cell.

See also Supplementary Videos 2 and 3.

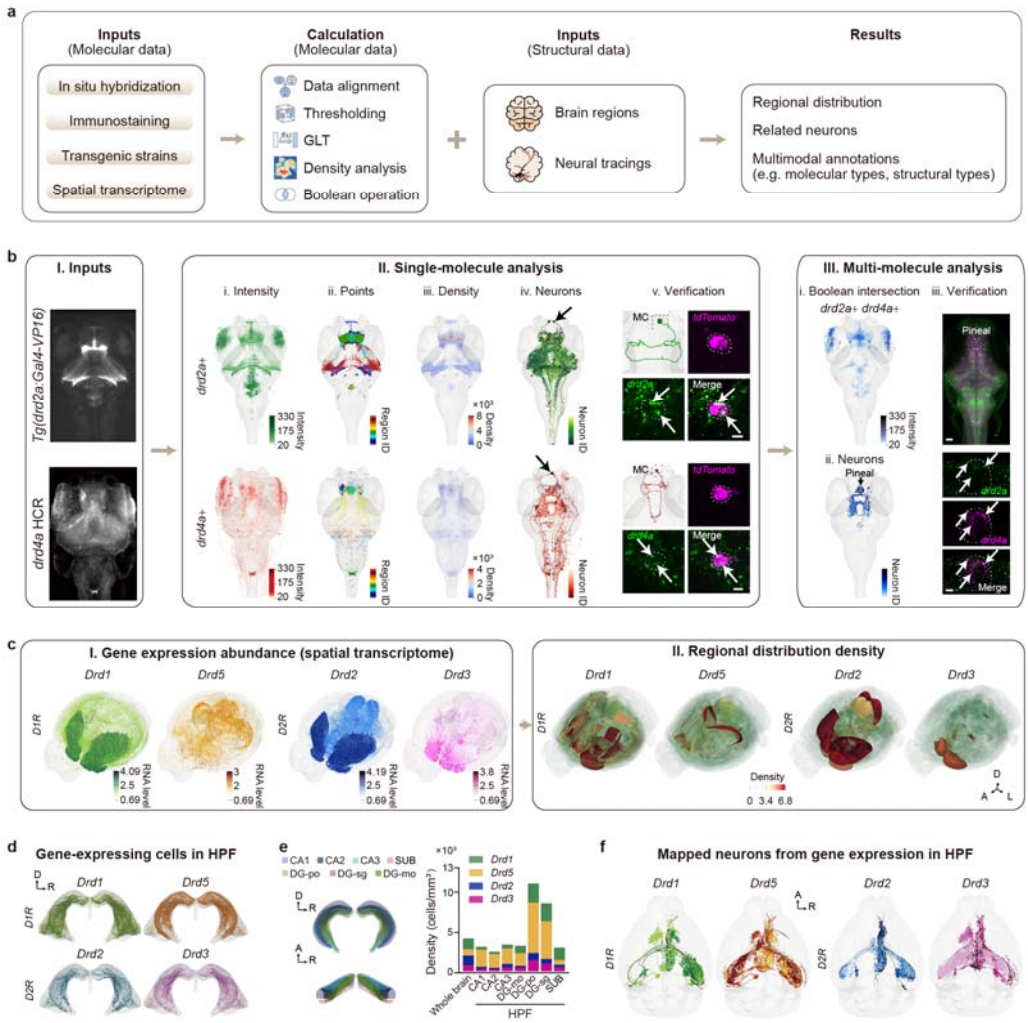

Fig. 4 | Mapping gene expression to neuronal morphology.

a, Workflow of gene-to-structure analysis. Registered gene expression images and spatial point data undergo various computational processes. Raw or intermediate outputs can be mapped onto structural datasets to reconstruct regional gene expression, identify gene-expressing neurons, and generate multimodal annotation.

b, Demonstration of gene-to-structure mapping using gene expression images. (I) Example raw images: *Tg(drd2a:GAL4-VP16)mpn211* fluorescence (top, crossed to *Tg(UAS:Dendra-kras)s1998t*) and *drd4a* HCR (bottom). (II) Single-molecule analysis: visualization as a 3D intensity image (i); digitization into spatial feature points, color-coded by regional distribution (ii) and density (iii); spatial mapping onto neuronal reconstructions to filter candidate neuronal tracings (iv), including two mitral cells (MCs, arrow); experimental validation of gene expression by HCR-FISH on the two MCs (v), which expressed tdTomato for morphology tracing (see Methods). Green puncta, HCR-FISH signals; white arrows, co-localization of HCR-FISH signals and tdTomato; dashed circles, outlines of MC somata. (III) Multi-molecule analysis: Boolean intersection (i) of the *drd2a* and *drd4a* expression images identified pineal gland neurons (arrow) co-expressing both genes (ii). HCR-FISH revealed the juxtaposition of *drd2a*$^{+}$ (green) and *drd4a*$^{+}$ (magenta) puncta within a single

optical plane in the pineal gland (dashed circle) (iii), supporting co-expression of *drd2a* and *drd4a* in pineal neurons. White arrows indicate co-expression puncta. Scale bars: 5 μm (II-v), 50 μm (III-iii, top), 10 μm (III-iii, bottom).

c, Mouse spatial transcriptomics visualized in BrAVe. (I) Expression abundance (normalized RNA counts) of dopamine receptor genes (*Drd1*, *Drd5*, *Drd2*, *Drd3*) at single-cell resolution.

(II) Region-wise density of receptor-expressing neurons ($\times 10^3$ cells per mm^3).

d, Spatial distribution of *Drd1*-, *Drd5*-, *Drd2*-, and *Drd3*-expressing neurons in the HPF.

e, Subregional organization of the HPF (left) and densities of receptor-expressing neurons in HPF subregions (right).

f, Volume rendering of mapped dopamine receptor-expressing neurons in the HPF.

A, anterior; D, dorsal; L, left; R, right. D1/2R, D1/2 dopamine receptor; HPF, hippocampal formation; GLT, gray level transformation.

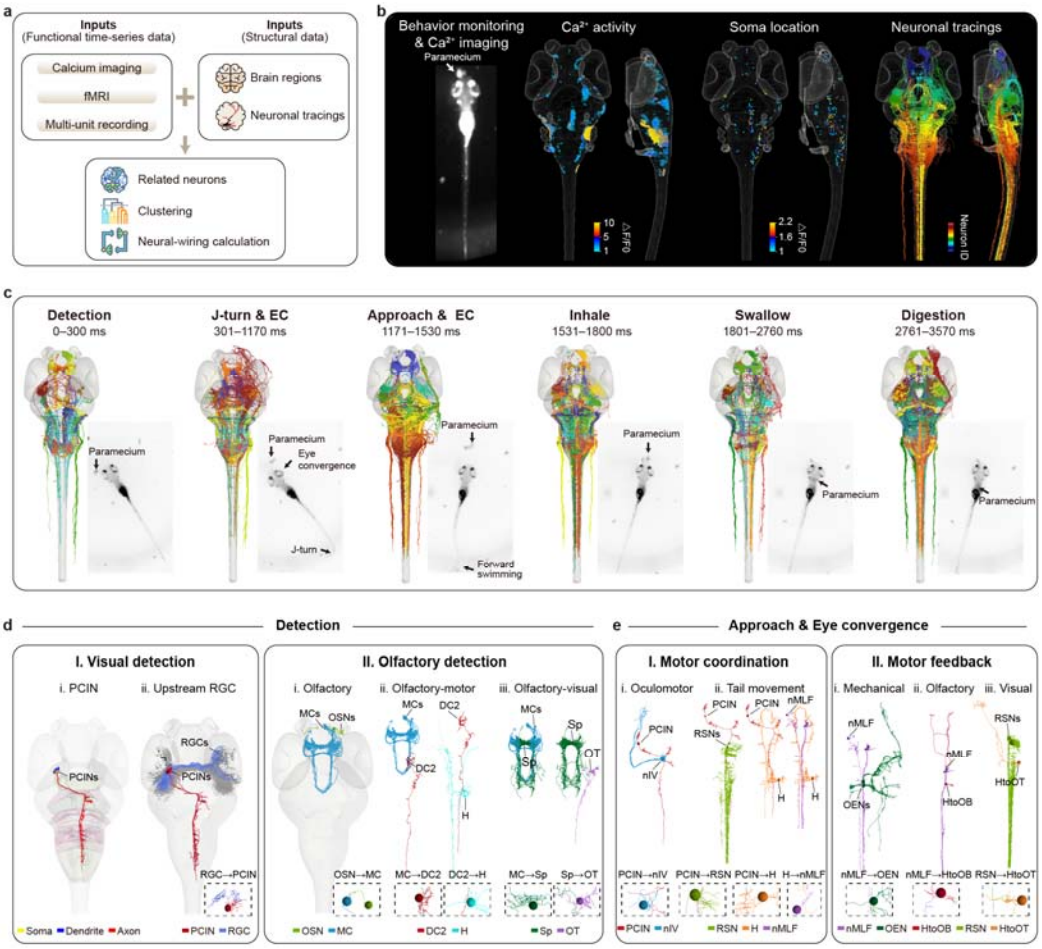

Fig. 5 | Mapping whole-brain neuronal activity to neural circuits.

a, Workflow of function-to-structure analysis. Registered functional imaging time-series (e.g. calcium imaging, fMRI) or time-series activity matrices of cells with spatial coordinates (e.g. multi-unit recording) can be imported into BrAVe to map corresponding neuronal tracings, cluster activated neurons, and identify associated neural circuits.

b, Multilevel alignment of behavior, functional activity, and neuronal tracings. Using the spatial correspondence function in BrAVe, brain-wide Ca^{2+} activity (second on the left, color coded by $\Delta F/F_0$) during prey-capture behavior (first on the left) was synchronously linked to soma positions (third on the left, color-coded by $\Delta F/F_0$ at each soma) and morphologies (right, color-coded by anteroposterior soma position) of activated neurons for integrated visualization.

c, Dynamic architecture of prey-capture circuits. Six behavioral epochs (detection, J-turn & eye convergence (EC), approach & EC, inhale, swallow, and digestion) are shown with morphologies of activated neurons, which are color-coded by excitatory and inhibitory morphotypes[14]. Bottom right, corresponding larval behavior and paramecium position.

d,**e**, Circuit dissection of prey detection (**d**) and approach & EC (**e**) epochs by neuronal wiring analysis. For prey detection, activated neurons include both visual (**d**-I, RGCs→PCIN) and olfactory (**d**-II-i, OSNs→MCs) pathways. Downstream of MCs, activated neurons engage

motor (**d**-II-ii, spinal cord-projecting DC2 and hindbrain neurons) and visual (**d**-II-iii, OT neuron via Sp) circuits. For approach & EC, downstream of PCIN, activated neurons include motor-related neurons for oculomotor (**e**-I-i, nIV) and tail movement (**e**-I-ii, RSNs and nMLF). Further downstream of RSNs and nMLF are hindbrain neurons projecting ascendingly to mechanosensory (**e**-II-i, OEN), olfactory (**e**-II-ii, HtoOB), and visual (**e**-II-iii, HtoOT) systems. Neuronal tracings are color-coded by morphotypes[14]. Dashed boxes highlight representative contacts between upstream and downstream morphotypes. DC2, diencephalic cluster 2; H, hindbrain; HtoOB, hindbrain-to-OB projecting neurons; HtoOT, hindbrain-to-OT projecting neurons; MC, mitral cell; nMLF, nucleus of the medial longitudinal fasciculus; nIV, trochlear nucleus; OEN, octavolateral efferent nucleus; OSN, olfactory sensory neuron; OT, optic tectum; PCIN, prey-capture initiation neuron; RGC, retinal ganglion cell; RSN, reticulospinal neuron; Sp, subpallium.
See also Supplementary Video 4.

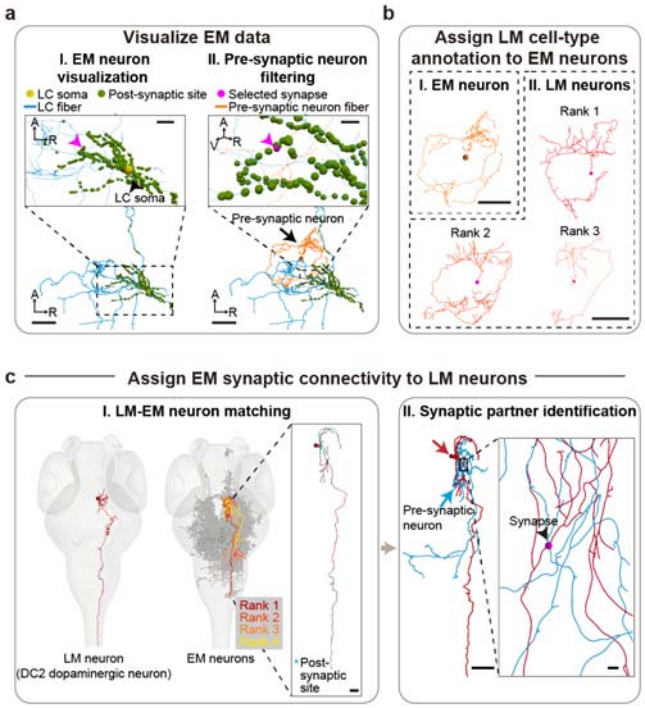

Fig. 6 | Bidirectional linking of LM and EM datasets through morphological matching.
a, Volume rending of an EM-reconstructed locus coeruleus neuron (yellow, soma; cyan, neurite; green, postsynaptic sites) (I), and co-rendering with a presynaptic partner (orange) filtered by a postsynaptic site (magenta arrowhead) (II). The black box in (II) shows a rotated and enlarged view of the inset (dashed rectangle), illustrating the selected postsynaptic site.
b, Filtered presynaptic neuron in **a** (I) and the three-highest scoring morphological matches from the LM structural atlas[14] (II). These LM neurons belong to a *vglut2a/2b*+ morphotype (# Glu-5L0701[14]) located in the dopaminergic diencephalic cluster 6.
c, Functionally defined prey capture-activated LM dopaminergic neuron in DC2 (I, left; see Fig. 5d, II-ii) and matched neurons (I, middle, color tracings) from the EM atlas (I, middle, grey tracings[15]). The top-matched EM neuron (rank1) is enlarged with postsynaptic sites in cyan (I, right). A presynaptic partner (cyan) of this rank1 EM neuron (red) was further identified, forming a single synapse (magenta) with it (II). Red and blue arrows indicate the somata of red and blue neurons, respectively.
Scale bars: 50 μm (**a**-I,II, **b**, **c**-II), 20 μm (**a**-I, inset), 5 μm (**a**-II, inset; **c**-I,II, inset). A, anterior; R, right; V, ventral. DC2, diencephalic cluster 2; EM, electron microscopy; LM, light microscopy.

Extended Data Figures and Legends

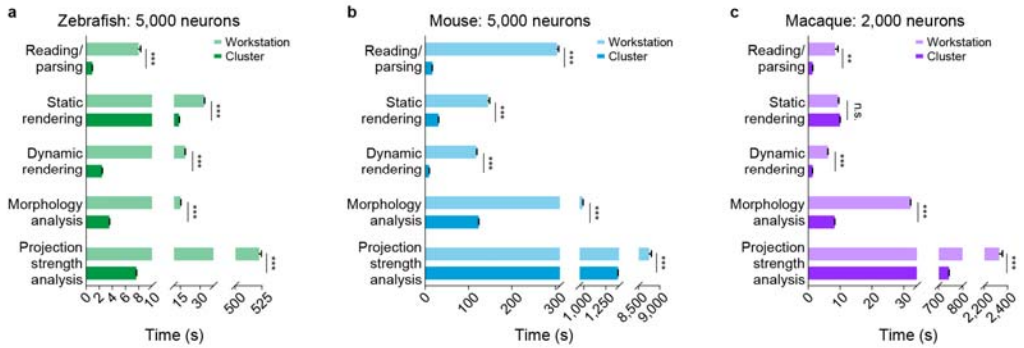

Extended Data Fig. 1 | Benchmarking BrAVe performance across operations and deployment modes.

a–**c**, Processing time for five operations—reading/parsing, static rendering, dynamic rendering, morphology analysis, and projection strength analysis—under standalone workstation (light) and computing cluster (dark) deployment modes, using neuronal tracing data from zebrafish (**a**, n = 5,000), mouse (**b**, n = 5,000), and macaque (**c**, n = 2,000). Bars show means from six independent runs, and error bars represent mean ± SEM. n.s., not significant; $^{**}P < 0.01$, $^{***}P < 0.001$ (two-way ANOVA with Sidak's post hoc multiple comparison test).